Electronic Supplementary Material (ESI) for Journal of Materials Chemistry A.
This journal is © The Royal Society of Chemistry 2015

Electronic Supplementary Information

Low voltage actuator using ionic polymer metal nanocomposites based on a miscible polymer blend

Varij Panwar,[a] Jin-Han Jeon,[b] Gopinathan Anoop,[a] Hyeon Jun Lee,[a] Il-Kwon Oh,[b] and Ji Young Jo*

[a] School of Materials Science and Engineering, Gwangju Institute of Science and Technology, Oryong-Dong, Buk-Gu, Gwangju 500-712, South Korea.

[b] School of Mechanical, Aerospace and Systems Engineering, Korea Advanced Institute of Science and Technology, 291 Daehak-ro, Yuseong-gu, Daejeon 305-701, South Korea.

*E-mail: jyjo@gist.ac.kr

Comparison of structure of blend membrane

For comparison of structure of P(VDF-TrFE)/PVP/PSSA and PVDF/PVP/PSSA the blend membrane, Fig. S1(a-b) shows the schematic structure of P(VDF-TrFE)/PVP/PSSA and PVDF/PVP/PSSA blends membranes, respectively. Fig. S1(a) shows uniform interaction of PSSA inside the backbone of P(VDF-TrFE) via PVP. Fig. S1(b) shows non-uniform of PSSA inside the backbone of P(VDF-TrFE) via PVP. Inset of Fig. S1(a-b) shows digital images of transparent solution of P(VDFTrFE)/PVP/PSSA/DMF blend and translucent solution of PVDF/PVP/PSSA/DMF blend, respectively.

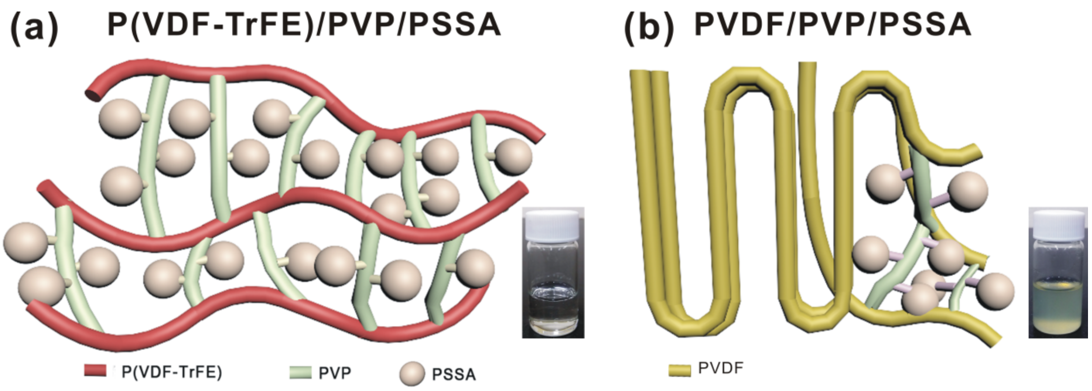

Fig. S1(a-b) Schematic structure of P(VDF-TrFE)/PVP/PSSA andPVDF/PVP/PSSA blend membranes, respectively. Inset of Fig. S1 (a-b) Digital images of P(VDFTrFE)/PVP/PSSA/DMF and PVDF/PVP/PSSA/DMF blend solutions

Electrochemical properties

Table S1 shows proton conductivity, IEC, and water uptake of both P(VDF-TrFE)/PVP/PSSA and PVDF/PVP/PSSA blend membranes with a blending ratio of 30/15/55 as well as the those of the commercial Nafion ionic polymer membrane.

Table S1. Electrochemical properties of ionic membrane.

Membrane	Water uptake	IEC (meq/g)	Proton conductivity (S/cm)
P(VDF-TrFE)/PVP/PSSA (30/15/55)	0.69	2.95	0.0065
PVDF/PVP/PSSA (30/15/55)	0.43	2.35	0.0011
Nafion	0.18	0.98	0.0047

Mechanical properties

The mechanical properties of the P(VDF-TrFE)/PVP/PSSA 30/15/55 blend membrane were compared with those of the PVDF/PVP/PSSA 30/15/55 blend membrane as well as Nafion membrane in the hydrated condition, as shown in Fig. S2 (a) and Tabulated in Table S2. The enhancement of Young's modulus, tensile strength, and maximum tensile strain of P(VDF-TrFE)/PVP/PSSA 30/15/55 blend membrane were observed, due to the strong intermolecular bonding among P(VDF-TrFE)-PVP, and PSSA-PVP acid-base pairs of P(VDF-TrFE)/PVP/PSSA blend membrane. Please note that the increase in Young's modulus of ionic membrane is beneficial for the actuation force of IPMNC. The DSC spectra of both PVDF and PVDF/PVP/PSSA blend membranes were shown in Fig. S2 (b), which depict the immiscible nature of PVDF/PVP/PSSA blend. The XRD patterns of both PVDF and PVDF/PVP/PSSA 30/15/55 blend membrane were shown in Fig. S2 (c), which show the weak intermolecular interaction between PVDF, PVP, and PSSA blends.

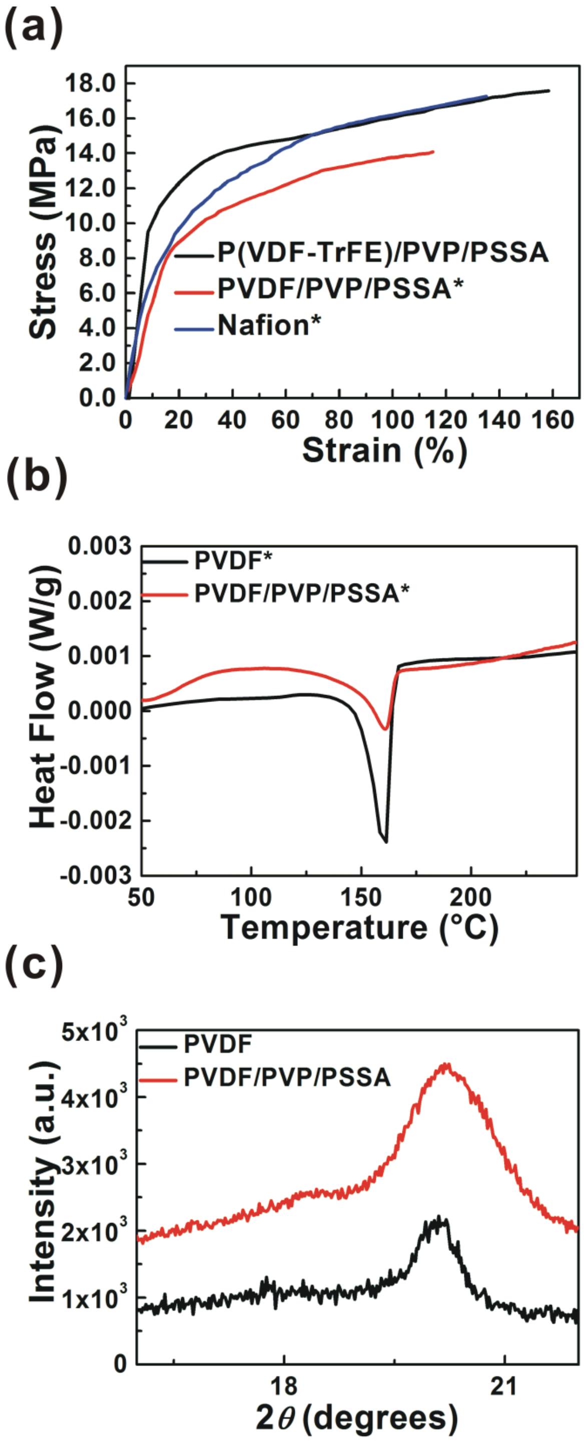

Fig. S2 (a) Stress as a function of stain for the P(VDF-TrFE)/PVP/PSSA membrane with a blending ratio of 30/15/55, PVDF/PVP/PSSA membrane with a blending ratio of 30/15/55, and the Nafion membrane, (b) DSC spectra and (c) XRD spectra of PVDF and PDVF/PVP/PSSA membranes with a blending ratio of 30/15/55. Asterisk (*) represents the result from [Ref.25]

Table S2. Mechanical properties of ionic membranes in the hydrated condition.

Membrane	Young's modulus(MPa)	Tensile strength(MPa)	Elongation at break(%)
P(VDF-TrFE)/PVP/PSSA (30/15/55)	117	17.6	158.3
PVDF/PVP/PSSA (30/15/55)	24	7.8	108.3
Nafion	74	17.3	135

Table S3 shows the assignment of the various wavenumbers corresponding to hydrogen bonding in our membranes.

Table S3. Assignment of FTIR absorption peaks for hydrogen bonding

Wavenumber (cm^{-1})	Assignment	Ref.
~1037, ~1186	SO_3H of PSSA - CO of PVP	49
~3454	OH of PSSA - CO of PVP	49
~1674	CO of PVP - SO_3H, OH of PSSA, C-C and CH_2 of P(VDF-TrFE)	50
~1282	C-C of P(VDF-TrFE) - CO of PVP	38
~1402	CH_2 of P(VDF-TrFE) - CO of PVP	38

Surface view of IPMNC

Fig. S3 shows the magnified top view of Pt electrode on P(VDF-TrFE)/PVP/PSSA membrane with a blending ratio of 30/15/55. The average particle size was estimiated around 10-20 nm.

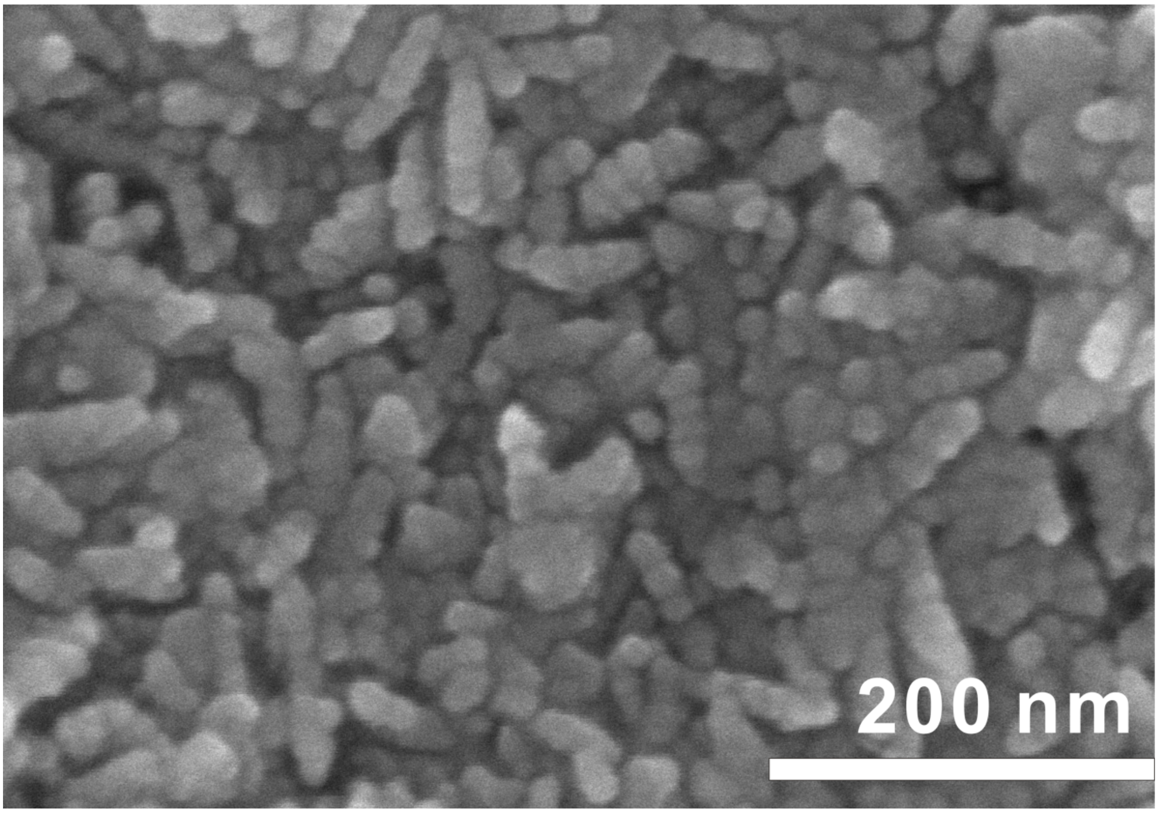

Fig. S3 High magnification top view SEM image of Pt-coated P(VDF-TrFE)/PVP/PSSA membrane with a blending ratio of 30/15/55.

TEM image of PVDF/PVP/PSSA blend membrane

The TEM images of PVDF/PVP/PSSA 30/15/55 blend membrane (Fig. S4) illustrates non-uniformly distributed pores structures and irregular wrinkled structure. The inset of Fig. S4 shows the high magnification of the selected area indicated using red square of PVDF/PVP/PSSA blend membrane shows planar structure.

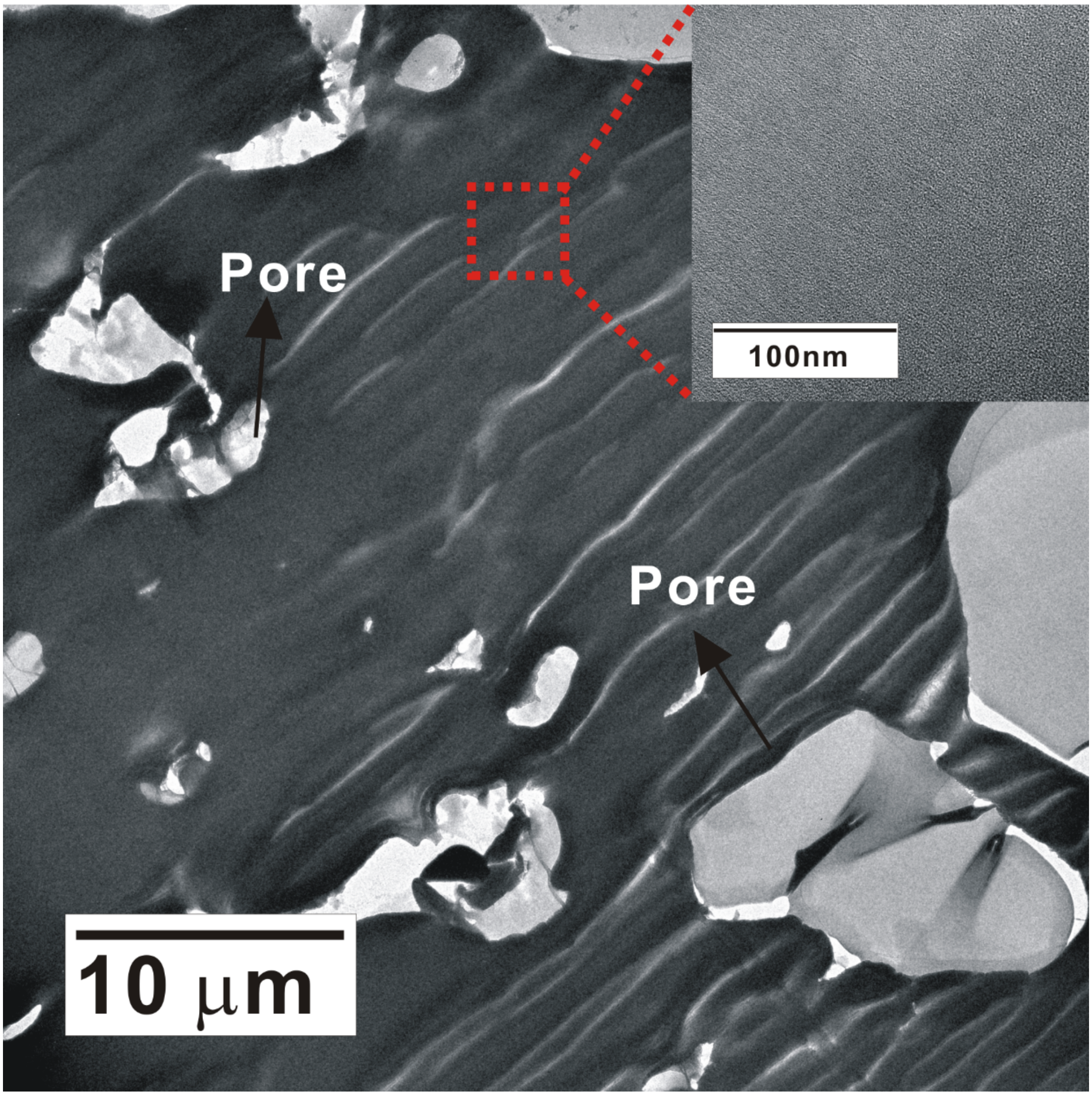

Fig. S 4 TEM images of the 30/15/55 blend membrane at magnification of x 500 and inset shows the magnified image of red box x 50000

Electrical properties

Fig. S5 depicts the current density-voltage curve of PVDF/PVP/PSSA based IPMNC. The dissipated electric power density and maximum current density of PVDF/PVP/PSSA IPMNC were evaluated to be 0.018 W/cm^2 and 0.015 A/cm^2 from this data.

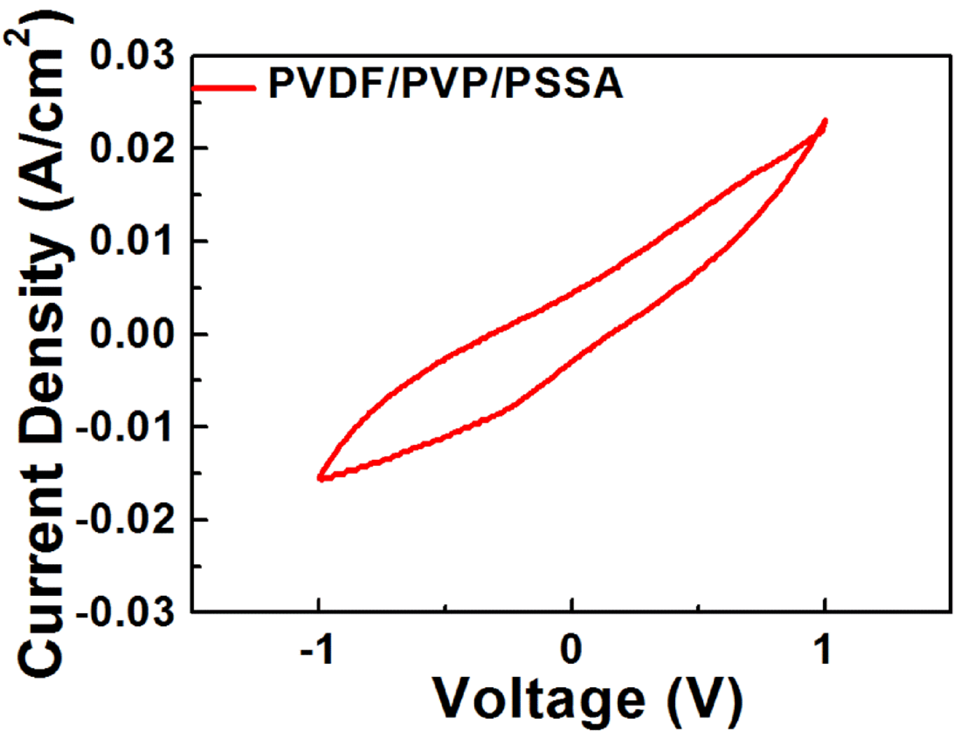

Fig. S5 Current density - voltage curve of PVDF/PVP/PSSA based IPMNC.

Table S4 shows surface resistance of IPMNC based on both the P(VDF-TrFE)/PVP/PSSA and the PVDF/PVP/PSSA blend membrane with a blending ratio of 30/15/55 as well as that of the commercial Nafion ionic polymer membrane.

Table S4. Surface resistance of IPMNC.

IPMNC	Surface resistance (Ω)
P(VDF-TrFE)/PVP/PSSA (30/15/55)	2
PVDF/PVP/PSSA (30/15/55)	3.5
Nafion	4

Actuation performance

Normalized displacement of PVDF/PVP/PSSA based IPMNC at DC voltage of 1 V in hydrated and dry condition is shown in Fig. S6(a). The actuation force of PVDF/PVP/PSSA based IPMNC at DC voltage of 1 V in the dry conditions is shown in Fig. S6(b). Normalized displacement of PVDF/PVP/PSSA IPMNC slowly increased with time due to the low proton conductivity and water uptake in hydrated condtion. In dry condition, normalized displacement of PVDF/PVP/PSSA increased with time sharply up to 10 s, after then it showed back-relaxation. The actuation force decreased with time after an intial increment. The normalized displacement of PVDF/PVP/PSSA IPMNC as a function of time at a frequency of 0.5 Hz under AC voltage of 1 V in hydrated and dry condition is shown in Fig. S6(c). The normalized displacement of PVDF/PVP/PSSA IPMNC as a function of frequency under AC voltage of 1 V in hydrated and dry condition is shown in Fig. S6(d) and its value decreased with an increase in frequency except the resonance frequency of 2 Hz and 7 Hz in hydrated and dry condition, respectively. The normalized displacement of PVDF/PVP/PSSA IPMNC in dry condition is found to be higher than in hydrated condition. This is due to the increased weight of IPMNC in hydrated condition (under water). The normalized displacement of PVDF/PVP/PSSA IPMNC as a function of number of cycles under AC voltage of 1 V in the hydration and the dry condion is shown in Fig. S6(e-f), respectively. In the hydrated condition, the normalized displacement increases up to 500 cycles, and then, it decreased with an increase in number of cycles. In the dry condition, the normalized displacement increases up to 50 cycles, and then, it decreased with an increase in number of cycles due to the low water uptake of PVDF/PVP/PSSA based IPMNC.

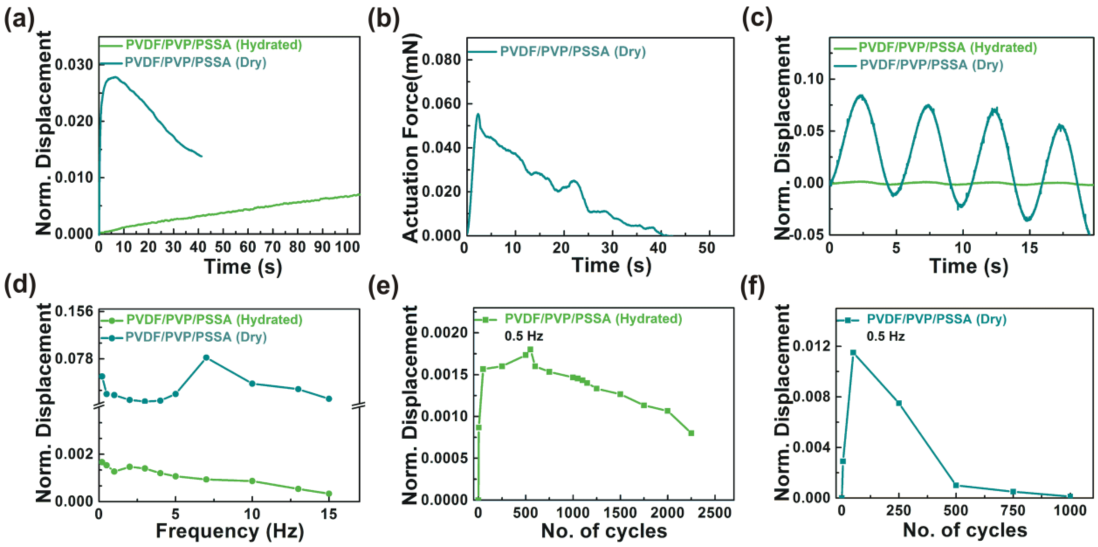

Fig. S6 (a) Normalized displacement of PVDF/PVP/PSSA -based IPMNC in a function of elapsed time under a DC voltage of 1 V in a hydrated and dry condition. (b) Actuation forces of PVDF/PVP/PSSA IPMNC in a function of elapsed time under a DC voltage of 1 V in a dry condition. (c) Normalized displacement of PVDF/PVP/PSSA IPMNC with time under AC voltage of 1 V. (d) Normalized displacement of PVDF/PVP/PSSA IPMNC in a function of frequency under AC voltage with an amplitude of 1 V. Normalized displacement of PVDF/PVP/PSSA IPMNC in a function of cycles under AC voltage with an amplitude 1 V (e) in the hydrated condition and (f) in the dry condition.